Journal of Aerospace Technology and Management
ISSN: 1984-9648
secretary@jatm.com.br
Instituto de Aeronáutica e Espaço
Brasil

Rodrigues Chaves, Flávio; Góis, José Carlos
Slow Cook-Off Simulation of PBX Based on RDX
Journal of Aerospace Technology and Management, vol. 9, núm. 2, abril-junio, 2017, pp. 216-221
Instituto de Aeronáutica e Espaço
São Paulo, Brasil

doi: 10.5028/jatm.v9i2.729

Slow Cook-Off Simulation of PBX Based on RDX

Flávio Rodrigues Chaves[1,3], José Carlos Góis[1,2]

ABSTRACT: Cook-off tests are commonly used to assess thermal behaviour of energetic materials under external thermal stimuli. Numerical simulation became a powerful tool to reduce the costs with experimental tests. However, numerical simulations are not able to predict the violence of thermal response, but instead accurately reproduce radial heat flow in the test vehicle and satisfactorily predict the delay time to ignition and ignition temperature. This paper describes the slow cook-off simulation of 3 selected PBX based on RDX in a small-scale test vehicle, using the equilibrium equation of Frank-Kaminetskii and testing 2 kinetic models: Johnson-Mehl-Avrami (n) and Šesták-Berggren (m, n). The influence of successive addition of binder elements (HTPB, DOS, and IPDI) on slow cook-off results of selected PBX was assessed. The variation of ±10% in input data was performed to determine the influence on the slow cook-off results. Results showed that the addition of binder elements reduces the delay time to ignition as well as ignition temperature and that the Šesták-Berggren (m, n) kinetic model generates smaller values and with less deviation linked to the variation of input data. The selection of kinetic model as well as the variation of ±10% in input data had a negligible influence on the slow cook-off results of cured PBX.

KEYWORDS: Thermal analysis, RDX, Activation energy, Kinetic model, Cook-off.

INTRODUCTION

Cook-off is the most common cause of accidents with energetic materials and ordnance items, being normally associated with dramatic consequences (Tobin 1994; Kummer 1996; Wada *et al*. 2004; Ministry of Ecology Sustainable Development Transport Housing 2012). It describes the response of energetic materials in weapon systems when exposed to abnormal thermal environments.

From the development of new energetic materials (EM) with high-energy content, the assessment of munition response to cook-off is very important to prevent and reduce the consequences of accidents. The enormous cost of experimental tests, particularly in large scale, leads to reduction in the number of tests that can be performed and consequently restricts the statistical significance of the results. In order to decrease the costs, numerical simulation is a suitable solution to predict the delay time (t) to ignition and ignition temperature of EM for different thermal scenarios. The development and validation of a kinetic model able to model cook-off are the major challenges in this field.

The purpose of this study was to determine the influence of kinetic models as well as thermochemical and kinetic parameters on the theoretical results of the slow cook-off (SCO) of 3 selected PBX based on RDX, using a commercial Abaqus 2D code (Abaqus 1998). The effect of successive addition of binder elements (HTPB, DOS, and IPDI) on the selected PBX is simulated in a SCO scenario, and the theoretical results are compared in terms of t for ignition and ignition temperature. Previous experimental results of t and ignition temperature obtained with a small-scale test vehicle (SSTV) (Chaves 2002) are used to validate kinetic models as well as thermochemical and kinetic parameters.

1.Associação para o Desenvolvimento da Aerodinâmica Industrial – Coimbra/Distrito de Coimbra – Portugal. **2.**Universidade de Coimbra – Departamento de Engenharia Mecânica – Laboratório de Energética e Detónica – Coimbra/Distrito de Coimbra – Portugal. **3.**Instituto Politécnico de Tomar – Unidade Departamental de Engenharia – Curso de Engenharia Mecânica – Tomar/Santarém – Portugal.

Author for correspondence: Flávio Rodrigues Chaves | Instituto Politécnico de Tomar – Unidade Departamental de Engenharia – Curso de Engenharia Mecânica | Quinta do Contador – Estrada da Serra | 2330-313 – Tomar/Santarém – Portugal | Email: flaviochaves@ipt.pt

Received: Jul. 04,2016 | **Accepted:** Dec. 23, 2016

COOK-OFF MODEL AND CHARACTERISTICS OF TEST VEHICLE

A numerical simulation of SCO was performed with a heating rate (HR) of 3.3 °C/h, according to STANAG 4383 and MIL-R-398A, based on the following equilibrium equation of Frank-Kamenetskii (Mader 1979; Victor 1997; Abaqus 1998; Dickson *et al.* 2000; Atwood *et al.* 2002; Suvranu 2011; Vyazovkin *et al.* 2011):

$$k\nabla^2 T + S = \rho c_p \frac{dT}{dt} \quad (1)$$

where: k is the thermal conductivity (W/m·K); T is the temperature (K); ρ is the density (kg/m^3); ∇^2 represents the Laplacian operator; c_ρ is the specific heat capacity (J/kg·K); t means time (s); S is the heat generation inside the system, which can be given by:

$$S = \rho q h(\alpha) A e^{-\frac{E}{RT}} \quad (2)$$

where: q is the heat of reaction (MJ/kg); $h(\alpha)$ is the empirical kinetic model function; A is the pre-exponential factor (1/s); E is the activation energy (kJ/mol); R is the universal constant (kJ/mol·K).

In order to establish a comparison with previous experimental SCO results (Chaves 2002), a SSTV of cylindrical shape with capacity of 1.57 cm^3 — internal diameter (id) = 10 mm and length (l) = 20 mm — was used for numerical simulation. Physical properties of the material used for the SSTV are presented in Table 1.

Table 1. Physical properties of the steel used for the SSTV.

Steel	Thermal conductivity, k (W/m·K)	Specific mass, ρ (kg/m^3)	Specific heat capacity, c_p (J/kg·K)
DIN 42CrMo4	42.7	7,900	460.9

NUMERICAL RESULTS AND DISCUSSION

Numerical simulation was performed using a 2-D symmetry plane of the SSTV and the finite element mesh shown in Fig. 1. A small mesh element with size of 0.5 mm was used near the wall of the test vehicle (Table 2 and Fig. 1) to increase the accuracy of the calculations of temperature and sharp pressure peaks that appear during an explosion. The element types used throughout the model were diffusion continuum axisymmetric 3 nodes (DCAX3) and diffusion continuum axisymmetric 4 nodes (DCAX4).

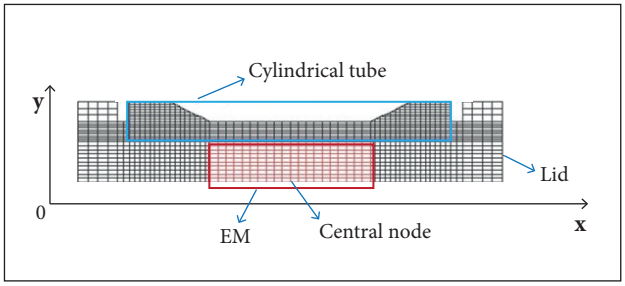

Figure 1. 2-D symmetry plane of SSTV and mesh size distribution.

Table 2. Mesh element size in EM and SSTV.

Material		Direction	
		Ox	Oy
EM		Uniform mesh with 1 node for each mm	Uniform mesh with 1 node for each 0.5 mm
SSTV	Cylindrical tube	Uniform mesh with 1 node for each mm	Uniform mesh with 1 node for each 0.5 mm
	Lid	Uniform mesh adequate to section	Uniform mesh with 1 node for each 0.5 mm

Heat transfer boundary condition around SSTV was governed by natural convection and radiation. Adopted values for the natural convection heat transfer coefficient and emission factor were 7.5 W/m^2·K and 0.8 (Incropera and De Witt 1990), respectively. The compositions of the 3 selected PBX used in this study are shown in Table 3.

Table 3. Composition of the 3 selected PBX based on RDX.

Reference	Composition (%, w/w)			
	RDX	HTPB	DOS	IPDI
PBX RH8515	85	15	-	-
PBX RHD8515	85	11.5	3.5	-
PBX RHDI8515	85	10.46	3.49	1.05

Between the EM and the SSTV no gap was considered, that is, the filling ratio was assumed ideal (100%). However, the existence of voids is a usual practice, which, according to some authors, can go up to about 10% (Jones and Parker 2004). The percentage of gap is usually used to provide adjusted results between simulations and experiments.

KINETIC MODELS AS WELL AS THERMOCHEMICAL AND KINETIC PARAMETERS

To characterize the influence of kinetic models on the theoretical results of SCO of the selected PBX, 2 kinetic models were tested (see Table 4), and the results of t to ignition and ignition temperature were used for comparison purposes.

Table 4. Kinetic models tested for numerical simulation of SCO of the selected PBX based on RDX.

Model	Symbol	$f(\alpha)$
Johnson-Mehl-Avrami (Šesták and Berggren 1971)	JMA (n)	$n\cdot(1-\alpha)\cdot[-\ln(1-\alpha)]^{1-(1/n)}$
Šesták-Berggren (Šesták 1984; Šesták 1993)	SB (m, n)	$\alpha^m\cdot(1-\alpha)^n$

Kinetic parameters were obtained using isoconversional methods, and non-isothermal kinetic analysis was based on differential scanning calorimetry (DSC) and thermogravimetry (TG) data. Friedman method (Friedman 1964), based on TG data, was selected to describe the thermal decomposition of RDX and PBX RH8515. For the other PBX (PBX RHD8515 and PBX RHDI8515) it was used the KAS method (Kissinger 1957; Akahira and Sunuse 1971), based on DSC data. The thermochemical and kinetic parameters used for numerical simulation are shown in Table 5.

In order to measure the importance of accuracy of thermochemical and kinetic parameters on the results of SCO simulation, a sensitivity test for ±10% in the input data was performed, and the influence on t for ignition and ignition temperature was evaluated.

RESULTS AND DISCUSSION

Numerical simulation performed for RDX was the starting point to study the addition effect of binder elements, and the results were used for comparative purposes. Figure 2 shows the

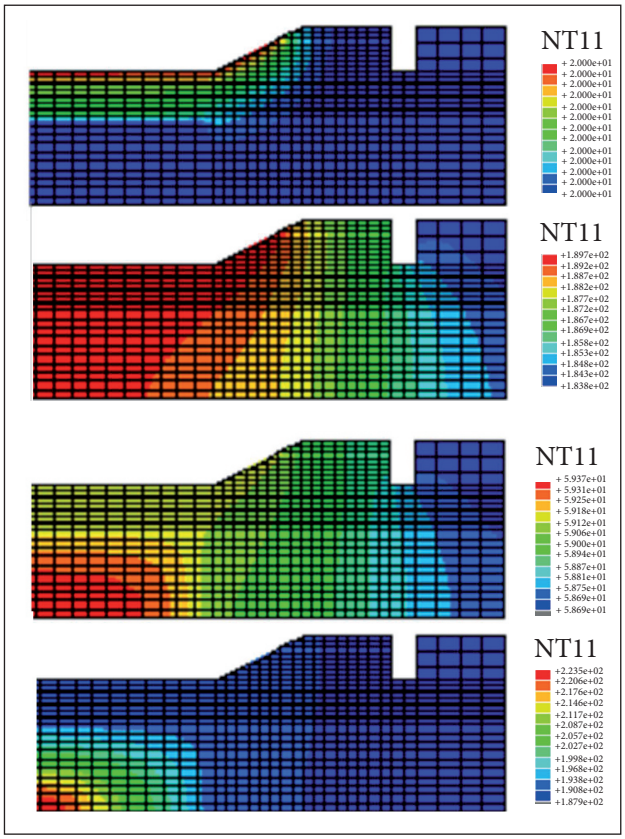

Figure 2. Temperature contour distribution in SSTV and PBX RHDI8515 in successive times during the SCO process.

Table 5. Thermochemical and kinetic parameters used as input data in the SCO simulation of selected EM.

Parameters	RDX	PBX RH8515	PBX RHD8515	PBX RHDI8515
Specific mass, ρ (kg/m^3)	1,800	1,564	1,565	1,569
Activation energy, E (kJ/mol)	189.67	156.26	168.44	269.32
Heat of reaction, q (MJ/kg)	2.002	2.446	2.076	1.540
Specific heat capacity, c_p (J/kg·K)	20 °C: 996.0 135 °C: 1,154.0	20 °C: 1,270.0 120 °C: 1,471.0 135 °C: 1,481.0	20 °C: 1,311.0 100 °C: 1,311.0 130 °C: 1,286.0	20 °C: 1,309.0 90 °C: 1,207.0 120 °C: 1,086.0
Thermal conductivity, k (W/m·°C)	20 °C: 0.260 160 °C: 0.203	20 °C: 0.255	20 °C: 0.255	20 °C: 1.110 48 °C: 1.090
Kinetic model SB (m, n) pre-exponential factor, A (1/s)	(0.242; 1.168) 3.34×10^{17}	(0.741; 0.335) 6.27×10^{13}	(0.570; 0.236) 8.79×10^{14}	(1.793; 1.434) 2.32×10^{27}
Kinetic model JMA (n) pre-exponential factor, A (1/s)	1.232 1.95×10^{17}	1.0 6.27×10^{13}	1.0 6.58×10^{14}	1.0 5.83×10^{26}

typical temperature contour distribution in the SSTV and PBX RHDI8515 at successive times during SCO process. As a result of the large difference between thermal conductivity of the SSTV and EM, the temperature increases evenly throughout the cylindrical wall of the SSTV up to a certain instant, from which heat generation arises inside the SSTV, driving to the ignition at the centre of the EM. The ignition at the centre of the EM occurred around 190 °C, when the difference between temperature of the cylindrical wall and the caps of the SSTV was around 40 °C.

Together, the slow HR and the small scale of test vehicle compel thermal decomposition to occur almost uniformly in a large area at the centre of the SSTV. Figure 3 show the mass decomposition (M) and temperature (T) profiles at the central node of SSTV for the kinetic models Šesták-Berggren (SB) (m, n) and Johnson-Mehl-Avrami (JMA) (n). The M and T profiles of EM are very similar for both kinetic models; however, it can be observed the influence of successive additions of binder elements, both on t for the onset of M and on t for ignition.

Table 6 shows the results of numerical simulation of SCO — t, M, and T — at the central point of SSTV, for RDX and the selected PBX based on RDX, allowing a comparative analysis between the kinetic models and a measurement of the influence of the addition of binder elements.

The results obtained for the 3 selected PBX show the influence of the successive additions of binder elements and the variation associated with the sensitivity test performed with ±10% of variation in input data (thermochemical and kinetic parameters). The results show: (a) t and T at the onset of M and (b) t for ignition, ignition temperature and M fraction at the onset of ignition.

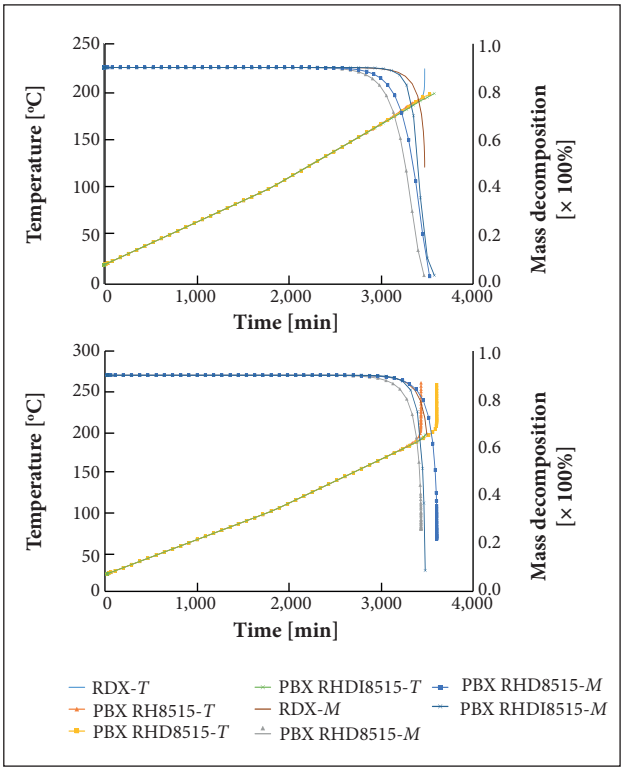

Figure 3. Profiles of temperature (T) and mass decomposition (M) at the central node of SSTV for SCO scenario. (a) using SB (m, n) kinetic model, (b) using JMA (n) kinetic model.

Table 6. Numerical simulation results of SCO (HR = 3.3 °C/h) of RDX and selected PBX based on RDX.

Onset of mass decomposition (1)			Onset of ignition (2)		
Kinetic model	Delay time (min)	Temperature (°C)	Delay time (min)	Temperature (°C)	Mass decomposition fraction (%)
RDX					
SB (m, n)	3,282.7	180.9	3,491.0	205.4	54
JMA (n)	3,357.2	185.5	3,487.7	197.6	65
PBX RH8515					
SB (m, n)	3,026.5 ± 84.8	167.1 ± 5.0	3,227.4 ± 35.7	179.6 ± 2.3	60.6 ± 5.5
JMA (n)	3,085.9 ± 99.7	170.4 ± 6.3	3,259.9 ± 79.2	181.7 ± 6.1	61.2 ± 6.7
PBX RHD8515					
SB (m, n)	3,078.3 ± 52.4	169.7 ± 3.0	3,246.7 ± 5.4	179.7 ± 0.3	70.7 ± 0.5
JMA (n)	3,162.2 ± 158.4	174.3 ± 8.8	3,333.6 ± 130.7	184.7 ± 7.5	71.2 ± 1.6
PBX RHDI8515					
SB (m, n)	3,221.2 ± 0.00	1,77.2 ± 0.00	3,447.5 ± 0.99	190.5 ± 0.99	63.9 ± 4.26
JMA (n)	3,221.2 ± 0.03	1,77.2 ± 0.00	3,444.5 ± 6.36	190.4 ± 0.23	58.1 ± 8.92

The numerical simulation results of SCO of RDX showed that *t* for ignition and ignition temperature obtained with SB (m, n) kinetic model was higher than that obtained with the JMA (n) one (3.3 min of difference for *t* and 7.8 °C of difference for ignition temperature). However, the delay time between the onset of mass decomposition and the onset of ignition was significantly lower when JMA (n) kinetic model was used, which corresponds to higher mass decomposition fraction (65 in opposition to 54%). Consequently a faster increase in pressure inside the test vehicle and a higher violence response of EM are expected.

The numerical simulation results of SCO obtained with both kinetic models showed that the addition of HTPB binder or/with DOS plasticizer to RDX decreased *t* and *T* at the onset of *M* and at the onset of ignition. This trend was higher when JMA (n) kinetic model was used.

When the IPDI curing agent was added the results of *t* at the onset of *M* and at the onset of ignition became closer to RDX, particularly when SB (m, n) kinetic model was used. However, regarding to ignition temperature the approach to RDX's results was not comparable.

When SB (m, n) was used, the addition of 15% (w/w) of HTPB to the RDX produced a reduction of 7.55% in the delay time to ignition and 12.6% in ignition temperature. When the 15% (w/w) of binder elements was the result of the HTPB addition (11.5%, w/w) and DOS (3.5%, w/w), the reduction in the delay time to ignition and ignition temperature was 7.0 and 12.5%, respectively.

When the JMA (n) kinetic model was used, the HTPB addition (15%, w/w) to RDX produced a reduction of 6.53 and 8.05%, respectively. Besides, when the 15% (w/w) of binder elements was the result of the HTPB addition (11.5%, w/w) and DOS (3.5%, w/w), the reduction was 4.41 and 6.53%, respectively.

When SB (m, n) kinetic model was used and the 15% (w/w) of binder elements was the result of the HTPB addition (10.46%, w/w), DOS (3.49%, w/w), and IPDI (1.05%, w/w), the reduction was 1.25 and 7.25%, respectively. When the JMA (n) kinetic model was used, the reduction was 1.24 and 3.64%.

The analysis of previous results about the influence of the addition of binder elements showed that the delay time to ignition predicted with both kinetic models is close. For the ignition temperature, a larger gap between the results of the 2 kinetic models was observed, being the minimum difference for the PBX RHDI8515 (3.61%) and the maximum difference for the PBX RHD8515 (5.98%).

The sensitivity test of ±10% in input data (thermochemical and kinetic parameters; see Table 5) produced less variation on the results of SCO of PBX RH8515 and PBX RHD8515 when the SB (m, n) kinetic model was used. When the PBX is cured (PBX RHDI8515), the effect of sensitivity test of ±10% in input data on the results of SCO was negligible for both kinetic models, except for mass decomposition results. This exception was higher when JMA (n) kinetic model was used.

In order to validate the more suitable kinetic model to describe the SCO of PBX based on RDX, simulation results of PBX RH8515 were compared with the experimental ones obtained in a SSTV made with the same material as well as the same geometry and size (Chaves 2002). The experimental results of SCO tests conducted with PBX RH8515 were performed with a HR close to 3.3 °C/h, used for numerical simulation. Table 7 shows the experimental results of the delay time to ignition and ignition temperature at the centre of SSTV.

Table 7. Experimental results of SCO test of PBX RH8515 in a SSTV (Chaves 2002).

Heating rate (°C/h)	Delay time to ignition (min)	Ignition temperature at the centre of SSTV (°C)
3.1	2,900.7	175.0
4.9	2,078.5	179.9

The delay time to ignition and ignition temperature are influenced by the HR. While the ignition temperature increased with the HR increasing, the delay time to ignition decreased. The simulation results of the delay time to ignition and ignition temperature obtained with SB (m, n) kinetic model showed a better approach with the experimental results than that obtained with the JMA (n) kinetic model.

If an interpolation of experimental results is conducted for HR = 3.3 °C/h, the difference between experimental and theoretical results for SB (m, n) kinetic model is 14.9 and 2.34% for the delay time to ignition and ignition temperature, respectively. If the results of sensitivity test of ±10% in input data are considered the difference of the delay time to ignition is between 13.6 and 16.2% and the difference on ignition temperature, between 1.03 and 3.65%. If the comparison is carried out with the theoretical results obtained with JMA (n) kinetic model the difference of the delay time to ignition and ignition temperature increases to 16 and 3.53%, respectively. Thus, if a variation of ±10% in input data is allowed, the theoretical results of both models are intercepted.

In order to improve the validation of kinetic models in future, the comparison should be conducted with experimental results

performed with the same HR, and an intermediate scale vehicle is recommended to move away the influence of the thermal conductivity from the cap to the centre of test vehicle by the thermocouple.

CONCLUSIONS

The numerical simulation of SCO of RDX and 3 selected PBX based on RDX was performed using Abaqus 2D code to determine the influence of binder elements on the SCO results of PBX and how much this influence is governed by the selection of kinetic model and variation of ±10% in input data (thermochemical and kinetic parameters).

For the same percentage of binder elements (15%, w/w) in PBX, the addition of HTPB binder alone or with DOS plasticizer produced the decrease in the delay time to ignition and ignition temperature. When IPDI curing agent was added to PBX, a significant increasing was observed in both results. The comparison of influence of kinetic models on the theoretical results of SCO of PBX RH8515 and PBX RHD8515 showed lower delay time to ignition and ignition temperature when SB (m, n) kinetic model was used. Nevertheless, when curing agent was added, the results became similar for both kinetic models.

A comparison with experimental results for PBX RH8515 showed a better approach to theoretical results when SB (m, n) kinetic model was used. The sensitivity test of ±10% in input data produced higher variation on the SCO results of PBX RH8515 and PBX RHD8515 and when JMA (n) kinetic model was used.

AUTHOR'S CONTRIBUTION

Both authors discussed the results and commented on the manuscript.

REFERENCES

Abaqus (1998) Manual do utilizador. Abaqus Standard. Pawtucket: Hibbitt, Karlson & Sorensen, Inc.

Akahira T, Sunuse T (1971) Joint convention of four electrical institutes. Research Report, Paper No. 246. Chiba: Chiba Institute of Technology.

Atwood AI, Curran PO, Bui DT, Boggs TL, Lee KB (2002) Energetic material response in a cookoff model validation experiment. Proceedings of the 12th International Detonation Symposium; San Diego, USA.

Chaves F (2002) Estudo do processo de decomposição térmica do explosivo plástico PBX RH8515 (Master's thesis). Coimbra: Universidade de Coimbra.

Dickson PM, Asay BW, Henson BF, Fugard CS (2000) Observation of the behaviour of confined PBX 9501 following a simulated cookoff ignition. Technical Report. Los Alamos: Los Alamos National Laboratory.

Friedman HL (1964) Kinetics of thermal degradation of char-forming plastics from thermogravimetry: Application to a phenolic plastic. Journal of Polymer Science: Polymer Symposia 6(1):183-195. doi: 10.1002/polc.5070060121

Incropera FP, De Witt DP (1990) Fundamentals of heat and mass transfer. 3rd ed. New York: John Wiley & Sons.

Jones DA, Parker RP (2004) Simulation of cookoff results in a small scale test. Melbourne: Explosives Ordnance Division, Aeronautical and Maritime Research Laboratory, DSTO.

Kissinger HE (1957) Reaction kinetics in differential thermal analysis. Anal Chem 29(11):1702-1706. doi: 10.1021/ac60131a045

Kummer PO (1996) EXADAT: a new explosives accident database. Proceedings of the 27th Department of Defense Explosives Safety Seminar; Las Vegas, USA.

Mader CL (1979) Numerical modeling of detonation. Berkeley: University of California Press.

Ministry of Ecology Sustainable Development Transport Housing (2012) Fireworks Accident Analysis. ARIA; [accessed 2017 Jan 18]. http://www.aria.developpement-durable.gouv.fr/wp-content/files_mf/Fireworksaccidentanalysis_jan2012.pdf

Šesták J (1984) Thermophysical properties of solids: their measurements and theoretical thermal analysis. Amsterdam: Elsevier.

Šesták, J (1993) Diagnostic limits of phenomenological models of heterogeneous reactions and thermal analysis kinetics. Solid State Ionics 63-65:245-254. doi: 10.1016/0167-2738(93)90113-H

Šesták J, Berggren G (1971) Study of the kinetics of the mechanism of solid-state reactions at increasing temperatures. Thermochimica Acta 3(1):1-12.

Suvranu D (2011) MANE 4240/CIVL 4240: introduction to finite elements. Abaqus 6.9SE Handout. Troy: Rensselaer Polytechnic Institute.

Tobin P (1994) Commercial explosives and their hazards. Washington: USEPA.

Victor AC (1997) Equations for predicting cookoff ignition temperatures, heating times, and violence. Propellants, Explosives, Pyrotechnics 22(2):59-64. doi: 10.1002/prep.19970220202

Vyazovkin S, Burnham AK, Criado JM, Pérez-Maqueda LA, Popescu C, Sbirrazzuoli N (2011) ICTAC Kinetics Committee recommendations for performing kinetic computations on thermal analysis data. Thermochimica Acta 520(1-2):1-19. doi: 10.1016/j.tca.2011.03.034

Wada Y, Nobe J, Ogata Y, Miyake A (2004) Relational Information System for Chemical Accidents Database (RISCAD) improved by addition of Thermal Hazard Data. Advanced Industrial Science and Technology; [accessed 2017 Jan 18]. http://www.rgipt.ac.in/title_doc/w-94.pdf